

Research on the Effect of Freeze–Thaw Cycles at Different Temperatures on the Pore Structure of Water-Saturated Coal Samples

Junwei Yuan, Jianxun Chen,* Yao Wang, Jingyi Xia, and Min Chen



Cite This: *ACS Omega* 2022, 7, 27649–27655



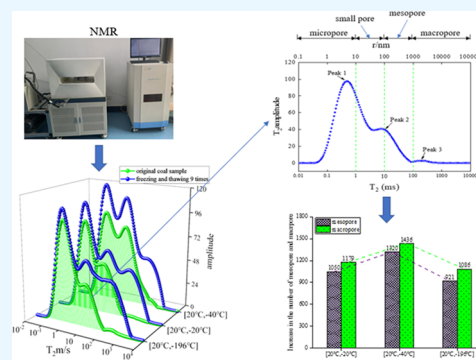
Read Online

ACCESS |

Metrics & More

Article Recommendations

ABSTRACT: To study the pore structure transformation of coal at different temperatures, freeze–thaw cycle experiments at different temperature intervals (20 to -20 °C, 20 to -40 °C, 20 to -196 °C) were carried out. The low-field nuclear magnetic resonance equipment was used to characterize the peak area, pore size distribution, and pore number of each group of coal samples. The pore transformation effect of coal samples at different temperature intervals was compared, and the change characteristics of the pore structure of coal samples under the freeze–thaw action were explored. The research shows that the freeze–thaw cycles at different freezing temperature intervals have obvious differences in the effect of coal pore transformation. The area of each peak spectrum in the T_2 distribution curve of coal samples increased significantly under the action of freeze–thaw cycles in different freezing temperature intervals. The increased value of the number of mesopores and macropores shows the phenomenon of “first increase and then decrease” with the increase of the temperature difference. There is a quadratic function relationship between the temperature difference in the freezing temperature interval and the proportion change rate of the adsorption pore or seepage pore. The continuous increase of the temperature difference has a certain marginal effect on the proportion change rate of seepage pores and adsorption pores in coal.



1. INTRODUCTION

Coal-bearing strata in China are generally affected by tectonic compression and shear stress, resulting in serious destruction of the coal seam structure and development of tectonic coal, forming the characteristics of poor permeability and difficult extraction of the coal seam.^{1–3} At the same time, hydraulic fracturing technology has been nearly perfected, but there are still various problems.⁴

Due to the heterogeneity and low thermal conductivity of coal, uneven thermal stress occurs in coal after freezing and thawing. At the same time, the water in the cracks of the coal sample freezes at low temperature and expands by 9.1% in volume.⁵ Therefore, the use of freeze–thaw cycles can damage the coal body, change the structural characteristics of the coal, and improve the gas extraction efficiency.

Domestic and foreign scholars have conducted extensive research on the cracking effect and influencing factors of freeze–thaw cycles. Scholars carried out the freeze–thaw cycle experiment on coal and rock and observed the evolution of the pore structure by means of nano-X-ray computed tomography (CT), nuclear magnetic resonance (NMR), and scanning electron microscopy (SEM), confirming the obvious indigenous transformation effect of the freeze–thaw cycle on the pore structure of coal and rock mass.^{6–10} In addition, the

calculation model of the frost heaving force under different conditions is deduced, and the numerical value of the frost heaving force produced by coal rock after freezing and thawing cycles is calculated. It is found that the magnitude of the frost heaving force is much larger than the tensile strength of coal rock, which confirms the remarkable transformation effect of freezing and thawing cycles on the pore structure of coal rock from a theoretical point of view.^{11–13}

With deepening research, scholars also noted that the effect of freeze–thaw cycles will be affected by various factors, such as the number of freeze–thaw cycles, the prefabrication temperature of coal samples, coal rank, moisture content, and the length of the cold shock. The effect of freeze–thaw cycles will have significant differences.^{14–19}

However, the experimental temperature is also an important factor affecting the effect of freeze–thaw cycles. Scholars' research focused on the evolution of the internal pore structure

Received: May 27, 2022

Accepted: July 13, 2022

Published: July 26, 2022



of coal samples under the conditions of cold–heat alternation, while few studies only considered the freezing temperature.^{20,21} Therefore, the authors will explore the pore evolution of saturated coal samples after experiencing the same number of freeze–thaw cycles from the perspective of different freezing temperatures.

2. METHODOLOGY

2.1. Preparation of Coal Samples. The coal samples were taken from the II₁ coal seam of the main coking coal industry in Anyang, and the specific location was 550 m away from the air inlet of the 2303 working face. The thickness of the coal seam is 2.22–8.53 m, and the average thickness of the coal seam is 5.67 m. The coal quality of the coal seam is coking coal, the apparent density is 1.33 t/m³, the average ash content of the raw coal is 15.65%, the average moisture content of the raw coal is 0.73%, and the volatile matter is 7.15–23.97%.

To ensure the similarity of coal sample properties, all the experimental coal samples are taken from the same coal block. The raw coal was cut into $\varnothing 25$ mm \times 50 mm cylinder samples using a Z5040 vertical drilling machine. The upper and lower end faces were polished smooth, and six coal samples without obvious cracks were selected. According to the different freezing temperature intervals, the coal samples were divided into three groups, two coal samples in each group. The grouping and numbering are shown in Table 1.

Table 1. Coal Sample Grouping and Numbering

experimental group	freezing temperature interval	group number
A	[20, –20 °C]	A1, A2
B	[20, –40 °C]	B1, B2
C	[20, –196 °C]	C1, C2

2.2. Experimental Equipment. The experimental system consists of three parts: nuclear magnetic resonance device, freeze–thaw cycle device, and auxiliary device (Figure 1).

2.2.1. NMR. The low-field nuclear magnetic equipment adopts the MseoMR23–060H-I low-field nuclear magnetic resonance experimental system produced by Suzhou New mai Technology Co., Ltd., including the host, display, test device, and test coil; this experiment chooses a 25 mm coil.

2.2.2. Freeze–Thaw Cycle Device. The liquid nitrogen refrigeration cycle system (–196 °C) mainly includes a liquid

nitrogen insulation barrel and freezing funnel. The JF/GDW-225L freeze–thaw cycle system (–20, –40 °C) mainly includes a special coal sample tank, freezing control system, and data acquisition and processing system.

2.2.3. Auxiliary Device. The auxiliary device is mainly composed of a vacuum water filling device, 2XZ-4 vacuum pump, GRX-9053 dryer, and electronic balance.

2.3. Experimental process.

- (1) Three groups of coal pillars were put in the drying oven, with the drying temperature set to 105 °C, drying to constant weight M ($M \pm 0.1\%$); then, each group of coal samples was put into a vacuum saturation device, and the vacuum pressure was adjusted to –0.1 MPa for 8 h. The T_2 distribution curve of the original coal sample under the saturated state was measured.
- (2) The coal samples of group A and group B after saturation were put into high- and low-temperature alternating boxes, and the freezing temperatures were set to –20 and –40 °C. After 30 min of freezing, they were taken out and completely thawed at room temperature (20 °C). Group C coal samples were put into the prepared funnel, and the funnel was frozen in an insulation bucket filled with liquid nitrogen for 30 min and then taken out to room temperature for complete thawing.
- (3) Step (2) was repeated to perform multiple freeze–thaw cycle experiments on three sets of coal samples. The T_2 distribution curve of each group of water-saturated coal samples after nine freeze–thaw cycles was determined.

3. RESULTS

The experimental results show that different freezing temperatures have obvious effects on the pore structure characteristics of coal. Given the limited length of the article, the most representative A1, B2, and C1 coal samples were selected for analysis.

3.1. T_2 Spectrum and Aperture Analysis. Nuclear magnetic resonance (NMR) can realize the qualitative and quantitative tests and analyses of internal pores in coal, which has the advantages of a wide detection range, short time consumption, and small damage to coal samples. The relationship between the transverse relaxation time T_2 and pore specific surface area of coal samples satisfies eq 1,^{22–24} where T_2 is the

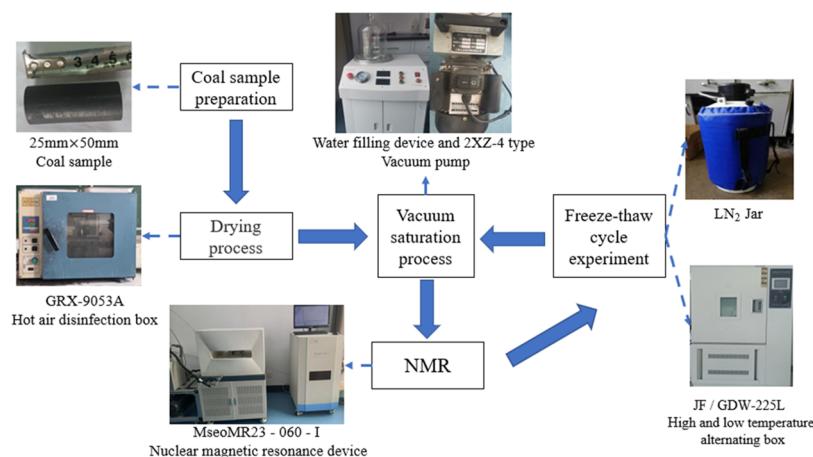


Figure 1. Experimental system.

transverse relaxation time; s is the pore surface area; v is the pore volume; and ρ is the transverse surface relaxation strength.

$$\frac{1}{T_2} = \rho \frac{s}{v} \quad (1)$$

Since the pore radius is proportional to the throat radius, eq 1 can be further simplified as eq 2, where F_s is the geometric shape factor and r is the pore radius.

$$\frac{1}{T_2} = \frac{\rho}{r} F_s \quad (2)$$

It can be seen from eq 1 that the transverse relaxation T_2 is proportional to the pore radius; the higher the transverse relaxation T_2 amplitude, the greater the number of pores relative to the pore size.²⁵ In this paper, the T_2 distribution curves of the original coal samples, and the nine freeze–thaw cycles at different freezing temperatures were obtained by NMR experiments, as shown in Figure 2.

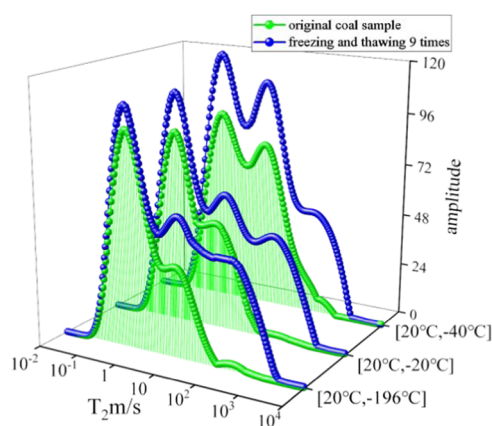


Figure 2. T_2 distribution curve of coal samples before and after freezing and thawing at different freezing temperatures.

It can be seen from Figure 2 that the T_2 spectra of the coal samples before and after the freeze–thaw cycle showed a significant “three-peak” structure, from left to right; the first peak, the second peak, and the third peak. By integrating the first, second, and third peaks of the three groups of the original coal samples in the T_2 distribution curve, the average peak spectral areas of the first, second, and third peaks of the three groups of original coal samples are 3363, 1931, and 65, respectively. The relationship between the transverse relaxation T_2 amplitude and pore radius shows that a smaller T_2 value corresponds to a smaller pore size, indicating that the number of small pores in the total pores of the original coal sample is large, and the number of mesopores and macropores is far less than that of small pores. After nine freeze–thaw cycles, the average peak areas of the first, second, and third peaks of coal samples at different freezing temperatures were 4166, 3012, and 2002, respectively. Compared with the original coal samples, after nine freeze–thaw cycles, the three-peak spectral area of the T_2 distribution curve of coal samples increased significantly; especially, the third peak spectral area increased 30.8 times, indicating that the freeze–thaw cycle can significantly improve the internal pore structure of the coal.

This paper adopts the classification results of B. B. Hodot on the pores in coal rock. The pore structure of coal can be divided into four categories: micropores ($r < 10$ nm), small pores ($10 < r$

< 100 nm), mesopores ($100 < r < 1000$ nm), and macropores ($r > 1000$ nm).²⁶

According to the corresponding relationship between the pore radius r of the coal sample and its transverse relaxation time T_2 in eq 2; for cylindrical pores, let F_s be 2 and ρ is 0.5×10^{-8} m/ms, and eq 3 is obtained.^{27,28}

$$r = 10^{-8} T_2 \quad (3)$$

Therefore, according to eq 3 and the classification of pores in coal and rock mass by B. B. Hodot, the T_2 distribution curve of coal samples can be processed to obtain the corresponding pore radius distribution curve. The corresponding pore radius distribution curve can be obtained by processing the T_2 distribution curve of coal samples. Figure 3 shows the T_2 distribution and pore size distribution curves of the original coal sample at this temperature by taking the temperature interval $[20, -196$ °C] as an example.

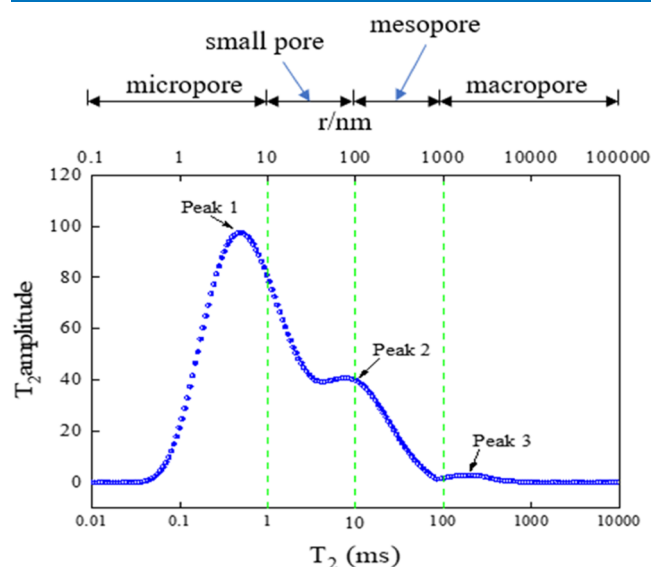


Figure 3. T_2 distribution and pore size distribution curve of the original saturated coal sample at $[20, -196$ °C].

The pore distribution curve was segmented and counted according to the classification method of B. B. Hodot’s pore diameter, and the change of the distribution proportion of various pore diameters of coal samples before and after freezing and thawing cycles at different freezing temperatures was obtained, as shown in Tables 2 and 3.

From the change of pore size distribution of coal samples, when the freezing temperature interval is $[20, -20$ °C], the ratio of the number of micropores, small pores, mesopores, and macropores of coal samples is 49:32:12:1, converted to 2.4:1.6:1.4:1; under the conditions of the freezing temperature interval of $[20, -40$ °C], the ratio of the number of micropores, small pores, mesopores, and macropores of coal samples was changed from 12:11:5:1 to 2:1.9:1.4:1; under the conditions of the freezing temperature interval of $[20, -196$ °C], the ratio of the number of micropores, small pores, mesopores, and macropores of coal samples was changed from 45:26:11:1 to 2.6:1.7:1.4:1.

The above-mentioned data show that the proportion of micropores and small pores in the original coal samples of three different temperature intervals is much higher than that of mesopores and macropores, indicating that the initial perme-

Table 2. Changes of the Pore Number of Coal Samples under Different Temperature Intervals

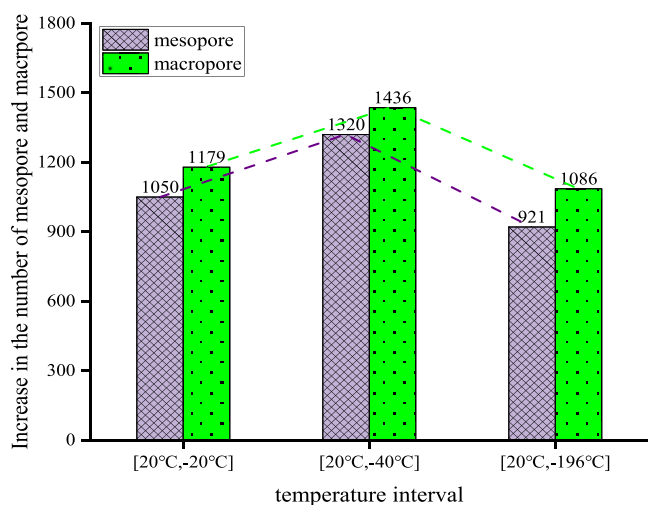
pore size	[20, −20 °C]			[20, −40 °C]			[20, −196 °C]		
	initial	final	increase	initial	final	increase	initial	final	increase
micropore	2428	2924	496	2445	3218	773	2639	2949	310
small pore	1582	1986	404	2316	3058	742	1552	1986	434
mesopore	622	1672	1050	1061	2381	1320	635	1556	921
macropore	50	1229	1179	208	1644	1436	59	1145	1086

Table 3. Change of the Pore Size Ratio of Coal Samples in Different Temperature Ranges

pore size	[20, −20 °C]			[20, −40 °C]			[20, −196 °C]		
	initial (%)	final (%)	rate of change (%)	initial (%)	final (%)	rate of change (%)	initial (%)	final (%)	rate of change (%)
micropore	51.86	37.43	−0.28	40.55	31.24	−0.23	54.02	38.62	−0.29
small pore	33.79	25.43	−0.25	38.41	29.69	−0.23	31.77	26.01	−0.18
mesopore	13.28	21.41	0.61	17.60	23.11	0.31	13.00	20.38	0.57
macropore	1.07	15.73	13.73	3.45	15.96	3.63	1.21	14.99	11.42

ability of the coal sample is poor and the gas extraction is difficult. After nine freeze–thaw cycles, the ratio of the pore size of coal samples in three temperature intervals changed greatly; especially, the number of mesopores and macropores increased significantly. The reason for the analysis may be that the frost heave force generated by the freeze–thaw cycle of the saturated coal sample in different temperature intervals promotes the formation of pores in the coal body, the number of pores increases significantly, and the micropores and small pores change to mesopores and macropores.

From the increase of the number of various pore size pores in coal samples, this paper obtains the change of the number of mesopores and macropores under different freezing temperature intervals, as shown in Figure 4.

**Figure 4.** Variation of the increment of the number of mesopores and macropores at different freezing temperatures.

It can be seen from Figure 4 that the number of mesopores and macropores of original coal samples and coal samples after nine freeze–thaw cycles in three different temperature intervals is positive. With the increase of the temperature difference in the freeze–thaw cycle temperature interval, the increase in the number of mesopores and macropores presents the phenomenon of “first increase and then decrease”. Under the experimental conditions, the freeze–thaw coal sample with the temperature interval of [20, −40 °C] has the best antireflection effect.

3.2. Change Analysis of Adsorption Pores and Seepage Pores. Based on the flow state of gas in the pores of different coal seams, pores can be divided into adsorption pores and seepage pores. The adsorption pore has a large specific surface area and strong gas adsorption capacity, which is an important place for gas adsorption. As the main channel of the gas flow, the seepage pore determines the efficiency and difficulty of coalbed methane mining. In the T_2 spectrum of coal samples, the part with $T_2 < 10$ ms is the adsorption pore and the part with $T_2 > 10$ ms is the seepage pore.²⁹ Therefore, the proportion of adsorption pores and seepage pores of the original coal sample and the coal sample after freezing and thawing nine times can be obtained, as shown in Table 4.

As can be seen from Table 4, after freeze–thaw cycles at different temperature intervals, the change rates of adsorption pores in each group are all negative, and the proportion of the adsorption pore volume in the total pore volume decreases, and the decreasing degrees are different in different freezing temperature intervals. Under the conditions of [20, −20 °C], [20, −40 °C], and [20, −20 °C], the proportion of adsorption pores decreased by 30.16, 28.44, and 16.09%, respectively. The change rates of seepage pores in each group of coal samples are positive, and the proportion of the seepage pore volume in the total pore volume increases, and the increase in amplitude is different at different freezing temperatures. Under the conditions of [20, −20 °C], [20, −40 °C], and [20, −20 °C], the proportion of seepage pores increased by 182.1, 169.7, and

Table 4. Changes in the Proportion of Adsorption Pores and Seepage Pores under Different Freezing Temperature Intervals

pore classification	[20, −20 °C]			[20, −40 °C]			[20, −196 °C]		
	initial (%)	final (%)	rate of change (%)	initial (%)	final (%)	rate of change (%)	initial (%)	final (%)	rate of change (%)
adsorption pore	85.6	61.3	−28.4	85.8	59.9	−30.2	74.0	62.1	−16.0
seepage pore	14.4	38.7	169.7	14.2	40.1	182.1	26.0	37.9	45.9

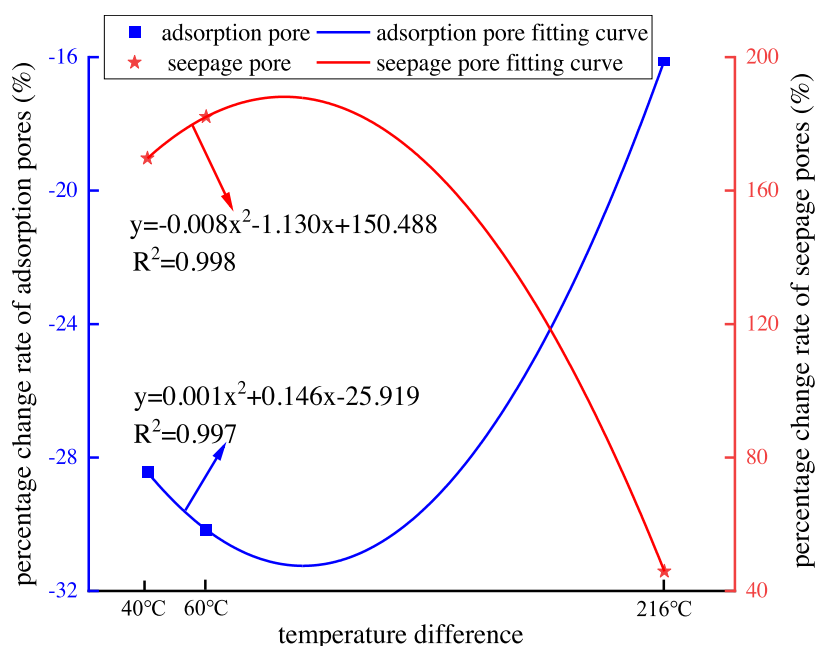


Figure 5. Change rate of the adsorption/seepage pore proportion under different temperature differences.

45.9%, respectively. After fitting analysis, the change rate of the proportion of adsorption pores and seepage pores in coal samples is an approximately quadratic function trend with temperature difference, as shown in Figure 5.

From the fitting curve in Figure 5, it can be seen that with the increase of temperature difference in the freezing temperature interval, the change rate of the pore proportion of seepage pores increases first and then decreases, while that of adsorption pores decreases first and then increases. Taking the seepage pore as an example, when the temperature difference of the freezing interval is low, the change rate of the seepage pore porosity will increase with the increase of the freezing temperature difference. When the temperature reaches the optimal freezing temperature of coal samples, the change rate of the proportion of seepage pores decreases with the decrease of the freezing temperature. The increasing temperature difference has a certain marginal effect on the change rate of the coal pore proportion. When the freeze–thaw cycle temperature exceeds a certain freezing temperature, the effect of the freeze–thaw cycles on the pore structure transformation of saturated coal samples begins to decline rapidly.

4. DISCUSSION

Under the action of freeze–thaw cycles, water-saturated coal samples not only generate thermal stress due to temperature changes but also have the frost heave force generated during the phase transition of water to ice. Existing research shows that compared with thermal stress, the frost heaving force is usually greater and determines the expansion of primary cracks in coal. Without considering the elastic deformation of the coal fissure wall and ice, ZHANG³⁰ believes that the frost heave force (P_f) of the water phase in coal to ice can be expressed as eq 4, where E_i and ν_i are the elastic modulus and Poisson's ratio of ice, respectively; n is porosity; β is the water–ice phase change volume expansion coefficient; ΔT is the temperature difference; and α is the coefficient of thermal volume expansion.

$$P_f = \frac{E_i[n\beta - \Delta T\alpha(1 - n)]}{3(1 - 2\nu_i)} \quad (4)$$

The porosity of coal samples A1, B2, and C1 is 7.65, 7.52, and 7.82%, respectively. The elastic modulus of ice is 600 MPa, Poisson's ratio is 0.35, the volumetric expansion coefficient of water–ice phase transition is 9%, and the thermal volumetric expansion coefficient of the coal sample is 2.5×10^{-6} .^{31–33} When the temperature difference is 40, 60, and 216 °C, the above-mentioned data is put into eq 4, and the frost heave force generated by the saturated coal sample is calculated to be 4.426, 4.668, and 4.351 MPa, respectively. The tensile strength of the coal sample in this paper is measured to be 2.45 MPa through experiments. It can be seen that the frost heave force generated by the coal sample after nine times of freezing and thawing under the conditions of three different freezing temperature intervals is greater than the tensile strength of the coal, and new pores in the coal sample are formed the original fissures further expanded, resulting in the structural damage to the coal body. According to the size of the frost heaving force, the frost heaving force is the largest under the temperature interval of [20, −40 °C], and the transformation effect of coal is the best. Under the conditions of the temperature interval [20, −196 °C], the frost heaving force is the smallest, and the transformation effect of coal is the worst, which is consistent with the experimental results. The difference of the frost heaving force under different temperature conditions also explains the characteristics of “increase first and then decrease” in the growth of medium and large pores and the quadratic growth of adsorption pores and seepage pores.

5. CONCLUSIONS

- (1) Under different temperature intervals, the peak area of saturated coal samples will increase in varying degrees, indicating that the internal pores of coal samples are further developed and the connectivity is enhanced.
- (2) After freeze–thaw cycles at different freezing temperatures, the number of pore sizes of coal samples increased significantly, in which the proportion of micropores and

small pores decreased and the proportion of mesopores and macropores increased. With the increase of the temperature difference in the freezing temperature interval, the number of mesopores and macropores increased first and then decreased.

- (3) The increasing temperature difference has a certain marginal effect on the change rate of the proportion of pores in the coal seepage pores. When the freeze–thaw cycle temperature exceeds a certain freezing temperature, the effect of freeze–thaw cycle on the pore structure transformation of saturated coal samples begins to decline rapidly. Therefore, it is of great significance to maintain the freezing temperature interval of coal during the freeze–thaw cycle for the cracking effect of coal.

AUTHOR INFORMATION

Corresponding Author

Jianxun Chen – School of Safety Science and Engineering, Henan Polytechnic University, Jiaozuo 454099, China; orcid.org/0000-0002-8189-6720; Email: 3184892680@qq.com

Authors

Junwei Yuan – School of Safety Science and Engineering, Henan Polytechnic University, Jiaozuo 454099, China; MOE Engineering Research Center of Coal Mine Disaster Prevention and Emergency Rescue, Jiaozuo 454000, China; Collaborative Innovation Center of Coal Work Safety and Clean High Efficiency Utilization, Jiaozuo 454003, China

Yao Wang – School of Safety Science and Engineering, Henan Polytechnic University, Jiaozuo 454099, China; orcid.org/0000-0001-7247-4019

Jingyi Xia – School of Safety Science and Engineering, Henan Polytechnic University, Jiaozuo 454099, China; orcid.org/0000-0001-5703-9828

Min Chen – School of Safety Science and Engineering, Henan Polytechnic University, Jiaozuo 454099, China

Complete contact information is available at: <https://pubs.acs.org/10.1021/acsomega.2c03306>

Notes

The authors declare no competing financial interest.

ACKNOWLEDGMENTS

This work was supported by the Key R&D and Promotion Projects in Henan Province (No. 202102310222).

REFERENCES

- YUAN, L. Strategic thinking on deep coal and gas co-mining in China. *J. China Coal Soc.* **2016**, *41*, 1–6.
- LI, Y.; PAN, S.; NING, S.; SHAO, L.; JING, Z.; WANG, Z. Coal measure metallogeny: Metallogenic system and implication for resource and environment. *Sci. China: Earth Sci.* **2022**, *65*, 1211–1228.
- LI, Y.; YANG, J. H.; PAN, Z. J.; MENG, S. Z.; WANG, K.; NIU, X. L. Unconventional Natural Gas Accumulations in Stacked Deposits: A Discussion of Upper Paleozoic Coal-Bearing Strata in the East Margin of the Ordos Basin, China. *Acta Geol. Sin.* **2019**, *93*, 111–129.
- SHEN, P. L.; LV, S. F.; LI, G. S.; REN, B.; BAI, J. P.; JIA, J. S.; CHEN, Z. Y. Hydraulic fracturing technology for horizontal wells in deep coalbed methane—a case study of Chang zhi North area of Qin shui Basin. *J. China Coal Soc.* **2021**, *46*, 2488–2500.
- QIN, L.; WANG, W. K.; LIN, H. F.; LIU, P.; LONG, H.; YANG, E. H.; LIN, S. H. Temperature evolution and freeze–thaw character-

istics of water-saturated-dried coal samples during low-temperature freeze–thaw process. *Fuel* **2022**, *324*, 124689–124697.

(6) SONG, Y. Q.; MA, H. F.; LIU, J. C.; LI, S.; ZHENG, J. J.; FU, H. Experimental study on uniaxial acoustic emission damage characteristics of freeze-thaw limestone. *J. Rock Mech. Eng.* **2022**, *41*, 2603–2614.

(7) QIN, L.; MA, C.; LI, S. G.; LIU, H. F.; DING, Y.; LIU, P.; WANG, P.; GAO, Z. Liquid Nitrogen's Effect on the Mechanical Properties of Dried and Water-Saturated Frozen Coal. *Energy Fuels* **2022**, *36*, 1894–1903.

(8) SONG, Y. J.; YANG, H. M.; TAN, H.; REN, J. X.; GUO, X. Study on damage evolution characteristics of sandstone with different saturation under freeze-thaw environment. *J. Rock Mech. Eng.* **2021**, *40*, 1513–1524.

(9) WANG, F.; CAO, P.; WANG, Y. Z.; HAO, R. Q.; MENG, J. J.; SHANG, J. L. Combined effects of cyclic load and temperature fluctuation on the mechanical behavior of porous sandstones. *Eng. Geol.* **2020**, *266*, 105466–105504.

(10) NIU, C. Y.; ZHU, Z. M.; ZHOU, L.; LI, X. H.; YING, P. D.; YU, Q.; DENG, S. Study on the microscopic damage evolution and dynamic fracture properties of sandstone under freeze-thaw cycles. *Cold Reg. Sci. Technol.* **2021**, *191*, 103328.

(11) DENG, Z. D.; ZHAN, X. X.; ZENG, W.; YANG, S. K.; WU, J. Q. A degradation model of mode-I fracture toughness of rock under freeze-thaw cycles. *Theor. Appl. Fract. Mech.* **2021**, *115*, 103073.

(12) CUI, G. Y.; MA, J. F.; WANG, X. L.; HOU, Z. A.; WANG, D. Y. Calculation method and engineering application of frost heaving force of broken surrounding rock tunnel in seasonal frozen area. *J. Southeast Univ.* **2021**, *51*, 294–299.

(13) LIN, H.; LEI, D. X.; YONG, R.; JIANG, C.; DU, S. G. Analytical and numerical analysis for frost heaving stress distribution within rock joints under freezing and thawing cycles. *Environ. Earth Sci.* **2020**, *79*, 227–238.

(14) MENG, F. D.; ZHAI, Y.; LI, Y. B.; LI, Y.; ZHANG, Y. S. Experimental study on dynamic tensile properties and energy evolution of sandstone after freeze-thaw cycles. *J. Rock Mech. Eng.* **2021**, *40*, 2445–2453.

(15) ZHANG, L.; TIAN, M. M.; XUE, J. H.; LI, M. X.; ZHANG, C.; LU, S. Effect of liquid nitrogen cycle treatment on seepage characteristics of coal samples with different water contents. *J. China Coal Soc.* **2021**, *46*, 291–301.

(16) YUAN, J. W.; WANG, Y.; CHEN, X. J. Study on the Evolution of Pore Structure of Anthracite Coal under Liquid-Nitrogen Freeze-Thaw Cycles. *ACS Omega* **2022**, *7*, 4648–4654.

(17) YAN, M.; ZHANG, Y. Z.; LIN, H. F.; LI, J. L.; QIN, L. Experimental study on damage characteristics of coal at different prefabrication temperatures by liquid nitrogen leaching. *J. China Coal Soc.* **2020**, *45*, 2813–2823.

(18) YUAN, J. W.; XIA, J. Y.; WANG, Y.; CHEN, M.; CHEN, J. X. Effect of Freeze-Thaw Cycles on Coal Pore Structure and Gas Emission Characteristics. *ACS Omega* **2022**, *7*, 16087–16096.

(19) WEI, Z. N.; ZHAI, C.; SUN, Y.; CONG, Y. Z.; TANG, W. Effect of liquid nitrogen cold shock duration on coal cracking. *J. China Univ. Min. Technol.* **2022**, *51*, 273–282.

(20) WANG, D. K.; ZHANG, P.; WEI, J. P.; YU, C. The seepage properties and permeability enhancement mechanism in coal under temperature shocks during unloading confining pressures. *J. Nat. Gas Sci. Eng.* **2020**, *77*, 103242.

(21) WANG, D. K.; ZHANG, P.; PU, H.; WEI, J. P.; LIU, S. M.; YU, C.; SUN, L. T. Microscopic CT experimental study on the evolution of coal fracture structure under temperature shock. *J. Rock Mech. Eng.* **2018**, *37*, 2243–2252.

(22) QIN, L. Study on pore structure evolution characteristics and permeability enhancement mechanism of liquid nitrogen cycle fracturing coal. *Beijing: China University of Mining and Technology*. 2018.

(23) SUN, X. T.; ZHOU, H. W.; XUE, D. J.; LIU, Z. L.; AN, L.; WANG, L.; CHE, J. NMR-based experimental study on self-absorption of low permeability coal. *J. China Univ. Min. Technol.* **2021**, *50*, 804–812.

- (24) YAO, Y. B.; LIU, D. M. Study on physical properties and fluid characteristics of shale reservoirs based on NMR relaxation spectroscopy. *J. China Coal Soc.* **2018**, *43*, 181–189.
- (25) ZHAI, C.; SUN, Y.; FAN, Y. R.; YANG, P. Q.; GE, X. M.; WU, W.; XU, J. Z.; YU, X.; LIU, T.; ZHAO, Y. Application and Prospect of Low Field Nuclear Magnetic Resonance Technology in Accurate Characterization of Coal Pore Structure. *J. China Coal Soc.* **2022**, *47*, 828–848.
- (26) ZHAO, J.; LIU, Z. Q.; KANG, Z. Q.; YANG, D. Study on the evolution law of permeability characteristics of oil shale in situ mining. *J. Rock Mech. Eng.* **2021**, *40*, 892–901.
- (27) CAI, C.; LI, G.; HUANG, Z.; et al. Experimental study of the effect of liquid nitrogen cooling on rock pore structure. *J. Nat. Gas Sci. Eng.* **2014**, *21*, 507–517.
- (28) XIE, S. B.; YAO, Y. B.; CHEN, J. Y.; YAO, W. Low Field Nuclear Magnetic Resonance Study on Pore Structure of Coal Reservoirs. *J. China Coal Soc.* **2015**, *40*, 170–176.
- (29) MA, H. T.; ZHAI, C.; XU, J. Z.; SUN, Y. Effect of ultrasonic frequency based on NMR technology on coal incentive fracturing effect. *Coal Geol. Explor.* **2019**, *47*, 38–44.
- (30) ZHANG, C. H.; ZHANG, H. X.; YU, Y. J.; LI, H. W.; WANG, L. G. Effect of saturation and redissolving on cracking of liquid nitrogen frozen coal. *J. China Coal Soc.* **2016**, *41*, 400–406.
- (31) LIU, H. Y.; ZHAO, Y. X. Theoretical calculation of frost heaving force of tunnel surrounding rock under freeze-thaw cycle. *J. Cent. South Univ.* **2020**, *51*, 1049–1058.
- (32) YIN, D. W.; CHEN, S. J.; XING, W. B.; HUANG, D. M.; LIU, X. Q. Experimental study on mechanical behavior of roof-coal pillar structure under different loading rates. *J. China Coal Soc.* **2018**, *43*, 1249–1257.
- (33) LIU, Q. S.; HUANG, S. B.; KANG, Y. S. Low temperature frozen rock single fracture frost heaving force and numerical calculation research. *Geotech. Eng.* **2015**, *37*, 1572–1580.